Journal of South American Earth Sciences 84 (2018) 208–222

Contents lists available at ScienceDirect

Journal of South American Earth Sciences

journal homepage: www.elsevier.com/locate/jsames

Quaternary sealevel changes and coastal evolution of the Island of Trindade, Brazil

Rodolfo José Angulo[a,*], Maria Cristina de Souza[a], Eduardo Guimarães Barboza[b], Maria Luiza Correa da Camara Rosa[c], Luiz Alberto Fernandes[d], Carlos Conforti Ferreira Guedes[e], Luiz Henrique Sielski de Oliveira[a], Rogério Portantiolo Manzolli[b], Sibelle Trevisan Disaró[f], Antonio Geraldo Ferreira[g], Caroline Maria Martin[d]

[a] Laboratório de Estudos Costeiros, Departamento de Geologia, Universidade Federal do Paraná, Centro Politécnico, Caixa Postal 19001, 81531-970 Curitiba, Paraná, Brazil
[b] Centro de Estudo de Geologia Costeira e Oceânica, Instituto de Geociências, Universidade Federal do Rio Grande do Sul, Brazil
[c] Departamento de Geodésia, Instituto de Geociências, Universidade Federal do Rio Grande do Sul, Brazil
[d] Laboratório de Estudos Sedimentológicos e Petrologia Sedimentar, Departamento de Geologia, Universidade Federal do Paraná, Brazil
[e] Laboratório de Estudos Costeiros, Departamento de Geologia, Universidade Federal do Paraná, Brazil
[f] Laboratório de Foraminíferos e Micropaleontologia Ambiental, Centro de Estudos do Mar, Universidade Federal do Paraná, Brazil
[g] Labomar, Instituto de Ciências do Mar, Universidade Federal do Ceará, Brazil

ARTICLE INFO

Keywords:
Coastal deposits
Holocene
Paleosea level
Beachrock
Vermetid-reef
South America

ABSTRACT

The present work presented the first dated paleosealevel indicators and new paleogeographic reconstructions of the Island of Trindade. All evidence for Holocene sealevels point to the elevations higher than the present in the age interval between 5.06 ka and 0.55 ka. The altitude and ages of the reconstructions are in good agreement with hindcast model curves and the empirical sealevel envelope for the mainland eastern and northeastern Brazilian coast. However, the position of paleo vermetid-reef indicates that sealevel was lower than eustatic elevation, suggesting an effect of island subsidence. In contrast to the Brazilian mainland coastal zone, where conspicuous evidences of Pleistocene highstands were recorded, no evidence of sealevels predating the Holocene has ever been observed on the island. This could be attributed to intense coastal erosion and log-term island subsidence.

A volcanic edifice rising more than 5500 m above the ocean floor was built by magmatic activity that extended over the late Pliocene and early Pleistocene. After the cessation of volcanic build up, the island started to shrink due to subaerial and marine erosion. During Pleistocene sealevel lowstands, alluvial fans were formed beyond the present limits of emerged areas. They were enclosed within and preserved from erosion by the Middle to Late Pleistocene lava flows and pyroclastic deposits. During Late Pleistocene sealevel highstand, intense coastal erosion removed the distal parts of the alluvial fans. It is very likely that at that time the entire coast of the island experienced intense erosion and subsidence as deduced from the absence of Pleistocene coastal deposits, which are widespread along mainland Brazilian coast.

The east coast of the island was dominated by high sea cliffs sculpted into volcanic rocks. A volcanic cone was subsequently formed, when the sealevel was lower than present during the Late Pleistocene to early Holocene. During the mid to late Holocene sealevel highstand the volcanic cone was partially eroded and a bay formed, where vermetid-reefs grow and sand beach deposits prograded until the bay was infilled. During the sealevel maximum, wave-cut terraces were formed and sea cliffs were active. During the lowering of the sealevel, cliffs became inactive and vermetid-reefs were eroded. Beach erosion and aeolian deflation presently prevails, indicating a low sediment supply.

* Corresponding author.
E-mail addresses: fitoangulo@gmail.com (R.J. Angulo), cristinasouza2527@gmail.com (M.C. de Souza), eduardo.barboza@ufrgs.br (E.G. Barboza), luiza.camara@ufrgs.br (M.L.C.d.C. Rosa), lualfernandes@uol.com.br (L.A. Fernandes), ccfguedes@gmail.com (C.C.F. Guedes), luizion@gmail.com (L.H.S. de Oliveira), rogeriomanzolli@gmail.com (R.P. Manzolli), stdisaro@ufpr.br (S.T. Disaró), geraldo@funceme.br (A.G. Ferreira), carolmartan@gmail.com (C.M. Martin).

https://doi.org/10.1016/j.jsames.2018.04.003
Received 25 September 2017; Received in revised form 28 February 2018; Accepted 4 April 2018
Available online 07 April 2018
0895-9811/

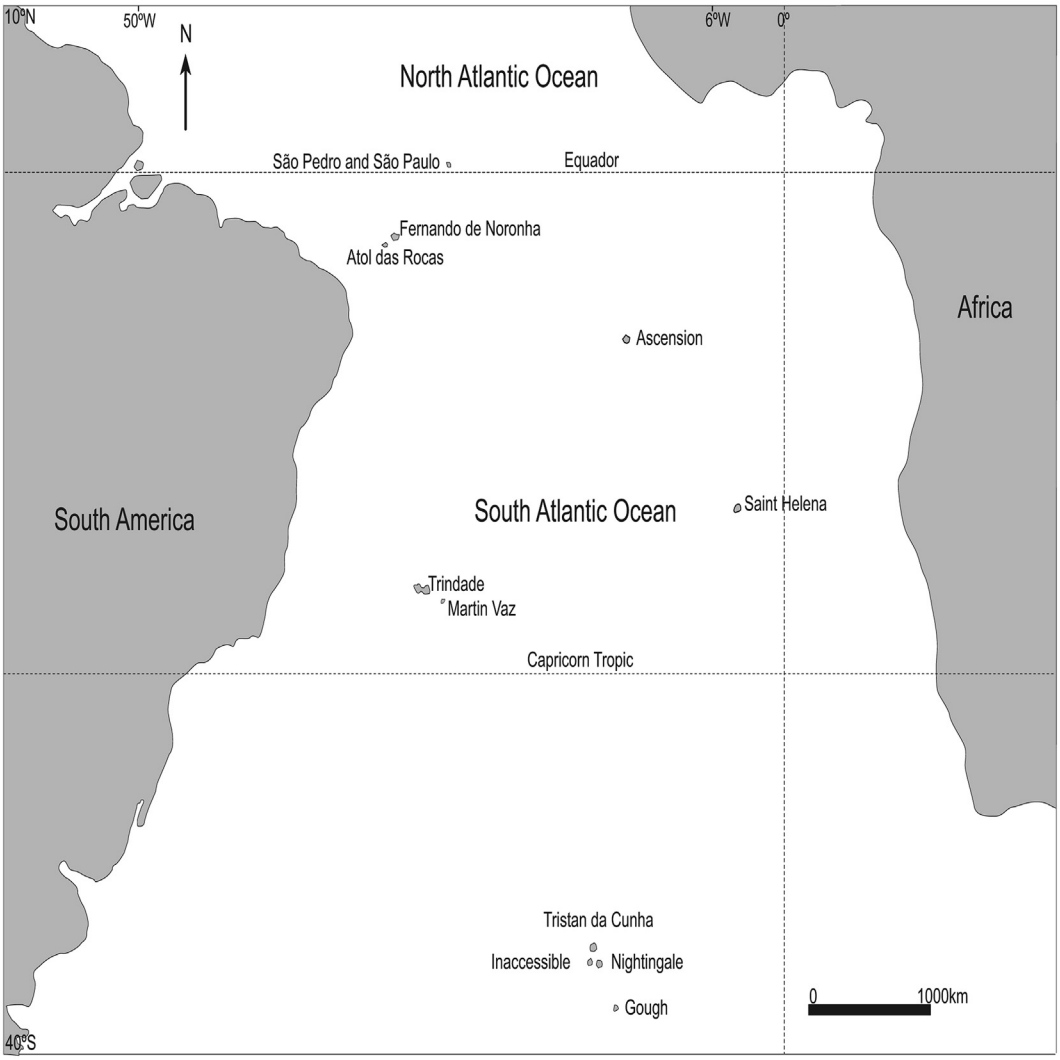

Fig. 1. South Atlantic oceanic islands between 0.9°N and 40.4°S.

1. Introduction

Evidence of sealevel changes obtained from remote oceanic islands are useful for reconstructing and for contributing to the understanding of global sealevel changes during the Quaternary and could help to solve issues related to the management of these islands. Until present the only references about sealevel changes and morphological and palaeogeographic IT evolution during the Quaternary are at the classic description of the geology written by Almeida (1961). There were recent advances in the studies of the recent geological past and sealevel changes on the other Brazilian oceanic islands, (i.e. Angulo et al., 2013 for Fernando de Noronha Archipelago and Angulo et al., 2013 for São Pedro and São Paulo Archipelago. The aim of the present work is to contribute to the understanding of Quaternary sealevel changes and to elucidate the coastal evolution of this isolated South Atlantic Ocean Island.

2. Study area

The Island of Trindade was discovered during the first decade of the 16th century (Lobo, 1919) and was occupied rarely and discontinuously until 1957, when the Brazilian Navy established a permanent base (Mayer, 1957).

The Trindade is a remote island located at 20.5°S, 29.3°W and 1140 km away from the Brazilian coast, except for Martin Vaz Island, 48 km away at 20.47°S, 28.51°W. The nearest islands are Fernando de Noronha (1870 km away at 3.85°S, 23.24°W), Atol das Rocas (1905 km, 3.87°S, 33.83°W), São Pedro and São Paulo (2370 km, 0.9°N, 29,4°S), Ascension (2125 km, 5.7°S, 7.9°W), Santa Helena (2540 km, 16.0°S, 5.7°W) and Tristan da Cunha (2475 km, 37.1°S, 12.3°W) (Fig. 1). With the exceptions of São Pedro and São Paulo, which are formed of a megamullion of mantle mylonitized rocks (Hekinian et al., 2000) all these islands are volcanic in origin (Darwin, 1839; Almeida, 1955, 1961; Gass, 1967; Nunn, 1984).

The classic description of the geology of the Island was written by Almeida (1961), and includes a 1:10,000 geological chart and extended petrographic data. According him, the islands of Trindade and Martin Vaz form the eastern end of the 1100 km long volcanic Vitória-Trindade submarine range (Fig. 2), and IT corresponds to the emergent portion of a Cenozoic alkaline volcanic edifice more than 5500 m high built up above the ocean floor. In the emergent portion, five volcanic units have been recognized: the Trindade Complex, the Desejado Sequence, the Morro Velho Formation, the Valado Formation, and Vulcão do Paredão. The Trindade Complex consists of Pliocene (Cordani, 1970) pyroclastic rocks, phonolite necks and intrusions of trachyandesites, nephelinites and alkaline ultrabasic rocks. The edifice presents four volcanic centres (Desejado, Morro Vermelho, Valado and Paredão) constituted by volcanic to subvolcanic subsaturated sodic–alkaline rocks (Almeida, 1961). The Desejado rocks yields K/Ar ages between 2.63 and 1.50 Ma and the Morro Vermelho ones ages lower than 170 ka (Cordani, 1970).

Fig. 2. The Victoria–Trindade submarine range (after Alves, 1998).

The Valado and Paredão centres are considered younger than Morro Vermelho and Paredão, which is the most recent volcanic event is estimated to have occurred during the Holocene (Almeida, 1961).

2.1. Quaternary sedimentary deposits

Almeida (1961) recognized eight sedimentary Quaternary units: (a) talus, (b) alluvial-fan deposits, (c) ancient sand and (d) gravel beaches, (e) present sand and (f) gravel beaches, (g) aeolian sands and (h) reefs (Fig. 3). The ancient beach deposits consist of sand, gravel, beachrocks and conglomerates.

2.2. Palaeosealevel

Almeida (1961) recognized geomorphological features and sedimentary deposits related to ancient sea levels. Almeida (1961) described dead sea cliffs at Bay of Portuguêses (Fig. 4) and at Bay of Príncipe, and a palaeo-wave-cut terrace at the Island of Rachada corresponding to a paleosealevel higher than the present one (Fig. 5). At Beach of Eme a wave-cut terrace ~3 m higher than the present one is covered by ~1 m of beach gravel (Almeida, 1961). In addition, a wave-cut terrace around Vulcão do Paredão is a maximum of 100 m wide at 3.0 m above mean sealevel; because waves can reach the terrace and remove debris that falls from the cliff; this feature was probably formed during the Holocene when the sealevel was higher than at present. Almeida (1961) also described outcrops of beachrock at the present beach face and at the storm-beach at Tartarugas and Andrada beaches at 3.5 m above mean sealevel, and inferred that these rocks were formed when the sealevel was higher than at present.

2.3. Climate and oceanographic parameters

The climate of IT is influenced by the South Atlantic Subtropical Anticyclone, which generates predominant weak and moderate winds from the east and northeast (Marinha do Brasil, 2011). The island is also influenced strong winds and swells from the south and southeast, mainly between April and September generate by cold fronts. The mean annual rainfall was 915 mm from 1963 to 1997; the wettest period is between April and June (110.5 mm mean monthly rainfall [mmr]), and the driest periods are between January and February (54.5 mm mmr) and August to October (55.9 mm mmr). The annual mean temperature is 26.3 °C: the mean monthly maximum of 30.2 °C occurs in February and the mean monthly minimum of 23.0 °C occurs in July. The archipelago experiences a semidiurnal microtidal regime, in which the mean spring and neap tidal amplitudes are 1.1 and 0.8 m, respectively (Marinha do Brasil, 2011).

3. Materials and methods

This paper provides descriptions of field morphological features and facies in outcrops and trenches, and the results of topographic levelling, ground-penetrating radar (GPR) profiles (Fig. 6), thin-section petrography, X-ray diffraction and radiocarbon dating. Also provides the wind rose based on daily 10 min wind data considering the period from October 28, 2012 to January 31, 2014, retrieved by the Automatic Meteorological Station, installed in the northeast side of the island at 20° 30′ 29″ S and 29° 18′ 57″ W.

Eleven carbonate samples were dated after acid etch pretreatment by radiocarbon Radiometric PLUS-Standard method and at Beta Analytic Inc. Miami, USA were analyzed (Table 1). The results were calibrated using the Calib Radiocarbon Calibration 6.0 program (Stuiver and Reimer, 1986).

Two tests were performed to determine the potential of the material for OSL dating, one on the bulk sample and the other after HCL (10%) treatment to remove carbonate clasts. All the tests were carried out using an automated Risø DA-20 TL/OSL system at the Luminescence

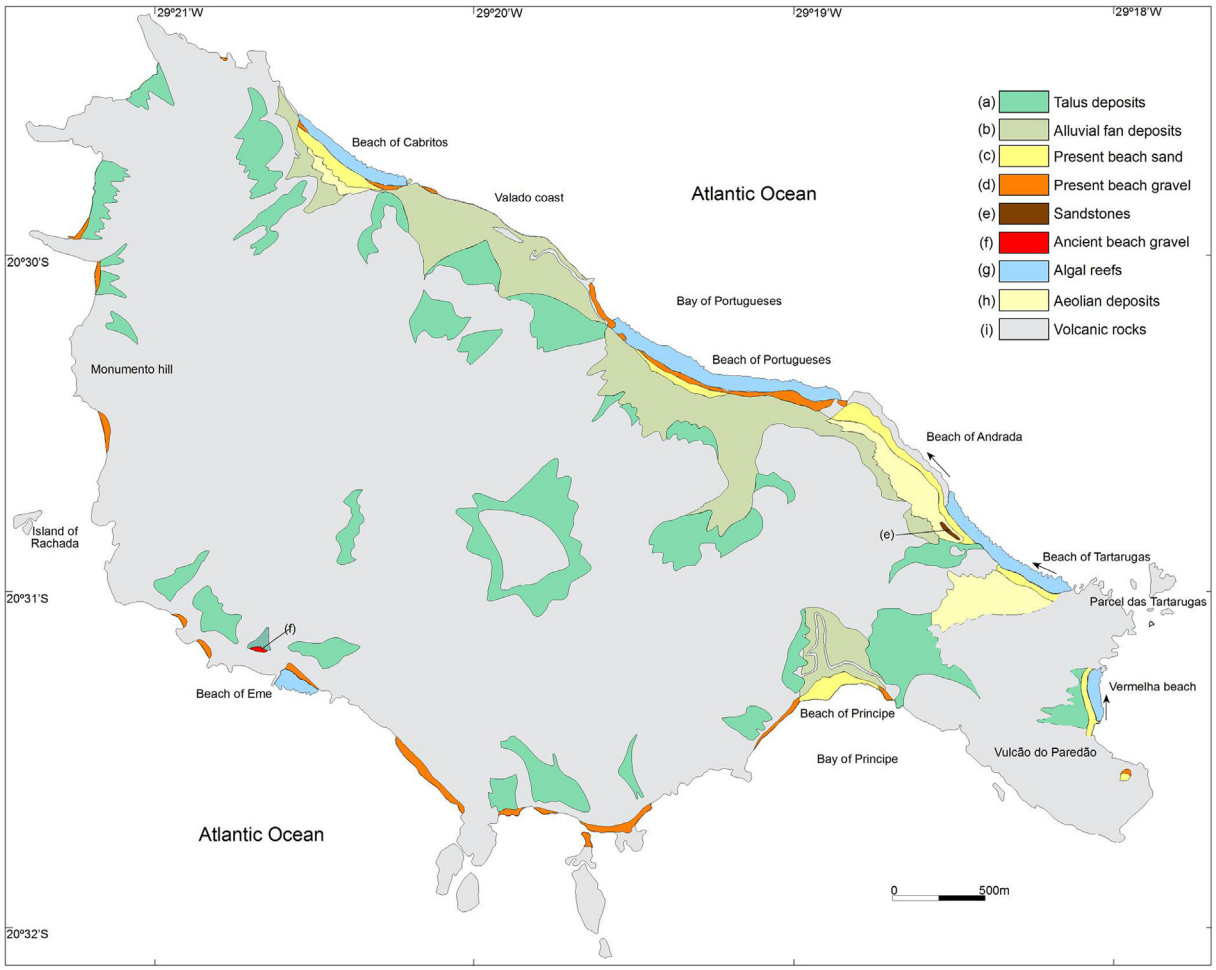

Fig. 3. Quaternary geological units on IT (after Almeida, 1961). Inferred predominant littoral drift (black arrows, this paper).

Fig. 4. High dead sea cliffs (c) at Beach of Cabritos beach formed by wave action over the distal part of the alluvial fan (f) deposits when the sealevel was higher than at present. (g) Foredunes.

Laboratory of Geosciences Institute of São Paulo University. The samples were analyzed to obtain the OSL and thermoluminescence (TL) signals after a given dose of 1 Gy, with no distinguishable signal in any case.

The GPR profiles (4919 m) were collected using the Common Offset method according Barboza et al. (2014). For a real-time topographic survey the GPR system was connected to a Global Positioning System (GPS). The GPR system comprised a GSSI™ (Geophysical Survey Systems, Inc.) SIR-3000 data collector with two antennas (400 MHz, GSSITM and 150 MHz, Radarteam Sweden AB), with a two-way traveltime (TWTT) range of 100–200 ns. This configuration enabled the penetration to a depth of 4–8.5 m. Noise and gain filters were applied at the time of data acquisition. Data were post-processed using Radan™, Reflex-Win® and Prism2® software packages, proceeding with background removal, bandpass frequency filters, Ormsby bandpass, gain equalization, topographic correction and time-to-depth conversion. A dielectric constant of 12 for wet sand was used to convert travel-time to depth, representing a velocity of 0.05 m/ns (Daniels et al., 1995). This constant was validated with lithological data obtained from trenches. GPR profiles were topographically corrected using GPS post-processed elevation data points collected along the profile lines at 1s time intervals. These data were acquired using a Trimble® PROXRS (datum: WGS84) and analyzed using a Geographic Information System (GIS). The GPS data were processed using the differential method, with the base station of the Brazilian Institute of Geography and Statistics located in the city of Vitória (Espírito Santo). The interpretation was based on the method of seismostratigraphy (Payton, 1977) adapted to GPR (Neal, 2004). This method was based on termination (onlap, downlap, toplap and truncations), geometry, and pattern of reflectors (Mitchum Jr. et al., 1977; Vail, 1977; Catuneanu et al., 2009; Abreu et al., 2010; Barboza et al., 2011).

Topographic profiles were acquired using a total station (Nikon, NIVO 2C). Level differences were measured in relation to a control point established in the area. The elevation of this point (25.85 m) was determined in relation to sealevel, by measuring the water line and

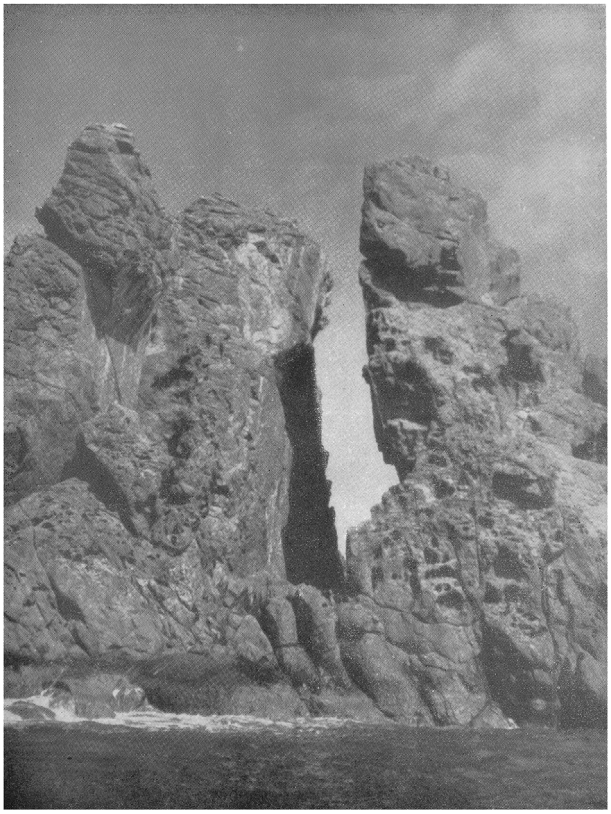

Fig. 5. Wave-cut terrace on the Island of Rachada (after Mayer, 1957) formed when the sealevel was higher than at present.

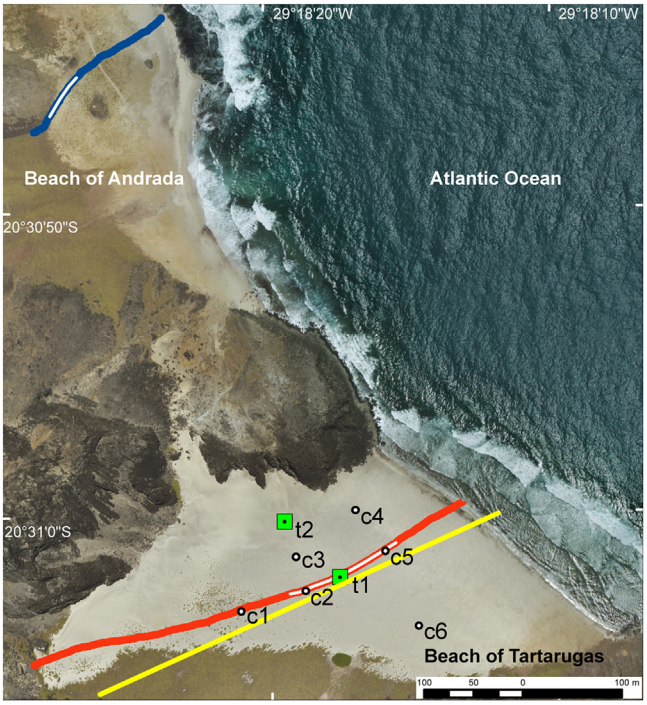

Fig. 6. Locations of trenches (t), cores (c), topographic levelling (yellow line) and GPR profiles at 150 MHz (orange line) and 400 MHz (blue line). White lines indicate the GPR sectors presented in Figs. 17 and 23. (For interpretation of the references to colour in this figure legend, the reader is referred to the Web version of this article.)

considering the tidal water level at that instant.

A topobathymetric digital model was established based on the Navy map at a scale of 1:15,000 (DHN, 1971). The distance between the level curves in the emergent area was 20 m, and the isobaths were at 5, 10, 20, 50, 100 and 500 m. To construct the model, the map was loaded into Esri® ArcMapTM, and its projection and datum were converted to UTM, WGS-84, Zone 26 South, and a georeference adjustment was conducted using GPS points and an orthophoto of the island. Subsequently, the contours were digitized and elevation/depth values were attributed to each line. Finally, the lines were converted into equidistant points that were interpolated using the natural neighbour method with a cell size of 10 m.

The characteristics and abundances of the constituents, matrix, cement and pores of rocks and sediments were estimated by visual analysis of thin sections using comparative charts from observations using polarized transmitted light microscopy. Scanning electron microscopy was carried out to examine very small features, objects, textures, grain relationships, matrix, cement characteristics and porosity. An energy dispersive analyser was also used for mineral identification and semi-quantitative chemical analysis. An Energy Dispersive Spectroscopy (EDS) system was used to produce element maps, which are useful for displaying element distributions in their textural context, particularly for highlighting compositional differences between grains and cements.

Paleosealevels were determined comparing the vertical range of occurrence of morphological, sedimentological and biological indicators whit the present homologous morphologic feature, facies or living specimens, according Angulo and Souza (2014).

4. Results

4.1. Winds

The winds recorded at the northeast coast of the Island blow predominantly from the east (E) much of the time, with strong winds from east-southeast (ESE) (Fig. 7) and predominance of weak winds from the north-northeast (NNE) direction. The absence of winds from southwest (SW), west-southwest (WSW), west (W) and, west-northwest (WNW) directions can be attributed to the station location, at sotavento of the island mountain, more than 600 m high. The wind speed increase from June to September when the South Atlantic Subtropical Anticyclone moves toward the coast of Brazil.

4.2. Geomorphology

The IT is a scarped volcanic hill approximately 6 km long, 2.5 km wide and 600 m high, with an area of 10 km^2. The shelf around the island is 1–3 km wide and 50 km^2 in area, with a slope of 1°30' to 7° and an abrupt break to 18°–30° at 100 m depth (Fig. 8).

Two distinct morphologies can be recognized on the IT. Most of the island is characterized by steeply sloping volcanicrock hills surrounded by large deposits of talus and alluvial fans and cones (Figs. 3 and 4). The southeast part of the island contains the volcanic cone Vulcão do Paredão, in which the crater and depositional volcanic slopes are partially preserved (Figs. 3 and 9). With the exception of this cone, the IT relief is the result of deep erosion of the volcanic edifice and several steep hills correspond to former volcano necks (Almeida, 1961). Talus and alluvial cone and fan deposits surround the steep erosional slopes: these deposits can extend as far as the coast (Figs. 3 and 4). In the northeastern part of the island Valado lava flows and pyroclastic rocks were deposited over the alluvial fans, thus preserving their sedimentary morphology (Fig. 4). The distal part of the fans has been eroded by wave action, which is still ongoing (Fig. 4). At the eastern end of the IT the asymmetry of the Tartarugas, Nossa Senhora de Lourdes, Vigia and Pão de Açucar hills is pronounced, suggesting that the steeper slopes were subjected to wave erosion and formed ancient sea cliffs in a palaeobay similar to presentday Baixio de Sueste Bay (Fig. 9).

Table 1
Radiocarbon datations and paleo-sea levels at IT.

Place	I	Latitude (S)	Longitude (W)	N	O	F	^{14}C a BP	^{14}C cal a BP	$\delta^{13}C_{PDB}$ (‰)	L	E (m)	H (m)	P (m)
Cabritos	C1	20°29′38″	29°19′52″	a	rr	r	3470 ± 40	3448–3244	−1.1	Beta-325,357	0.5–0.6	1.3–1.4	> 1.3
Valado	V1	20°29′44″	29°19′36″	a	b	bf	4010 ± 40	4144–3889	+0.3	Beta-325,358	1.4–1.5	(-0.8)-2.0	0.6 ± 1.4
Andrada	A1	20°30′53″	29°18′24″	s	br	bf	2430 ± 30	2140–1990	+2.5	Beta-376,954	0.7–1.3	(-1.2)-1.5	0.2 ± 1.4
Tartarugas	T1	20°30′56′	29°18′12″	s	br	bf	3040 ± 40	2913–2728	−1.2	Beta-325,355	–	–	–
Tartarugas	T2	20°30′56″	29°18′12″	a	b	bf	3290 ± 40	3261–2988	−3.6	Beta-325,356	–	–	–
Tartarugas	T3	20°31′00″	29°18′16″	a	b	bf	1070 ± 40	701–547	−8.9	Beta-325,357	1.2–1.3	(-0.2)-0.2	0.0 ± 0.2
Tartarugas	T4	20°31′00″	29°18′14″	a	rr	r	3580 ± 30	3550–3395	−0.1	Beta-376,957	0.2	1.1–1.5	1.3 ± 0.2
Tartarugas	T5	20°31′00″	29°18′14″	c	b	bf	3700 ± 30	3620–3605	+0.3	Beta-376,956	0.3	1.1–1.5	1.3 ± 0.2
Tartarugas	T6	20°31′02″	29°18′10″	a	rr	r	4750 ± 30	5060–4885	−0.2	Beta-376,960	- 0.3	0.6	> 0.6
Tartarugas	T7	20°31′02″	29°18′10″	a	rr	r	4150 ± 30	4310–4135	−0.8	Beta-376,959	- 0.6	0.6	> 0.6
Parcel das T	P1	20°31′05″	29°18′04″	s	br	bf	2720 ± 30	2490–2335	+1.8	Beta-376,955	2.2–2.8	(-0.3)-3.0	1.4 ± 1.7

Notes: (I) sample identification (N) sample nature, (O) occurrence, (F) facies, (^{14}C a BP) radiocarbon years before present, (^{14}C cal a BP) radiocarbon calibrated years before present, (L) laboratory reference, (E) elevation above mean-sealevel, (H) elevation relative to present homologous level, (P) paleosealevel; (a) calcareous red-algae, (s) calcareous sandstone, (c) coral, (rr) reef remain, (b) bioclast, (br) beachrock, (r) reef, (bf) beach-face.

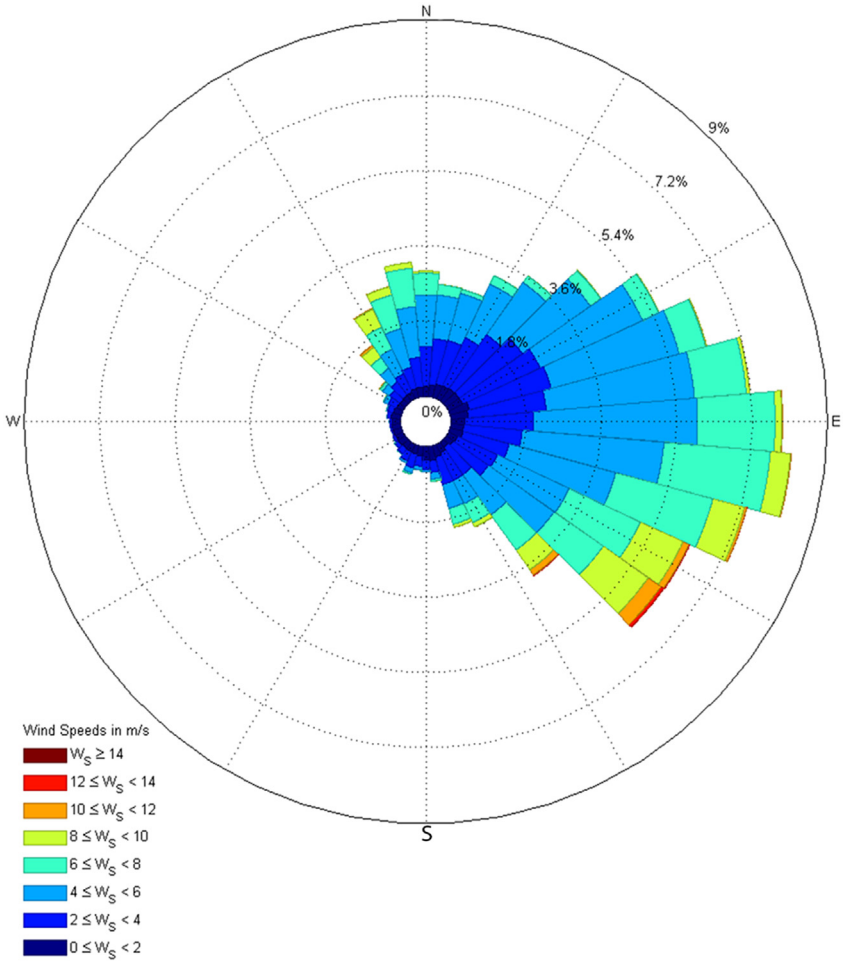

Fig. 7. Wind directions and speeds from October 28 2012 to January 31 2014 recorded by meteorological station locate at the northeast coast of the Island of Trindade.

The coast of the IT is dominantly erosional, with cliffs that can reach heights of ~200 m (Figs. 9 and 10). Conspicuous wave-cut terraces can be observed at Vulcão do Paredão, Parcel das Tartarugas, and other places along the IT coast (Fig. 10). Beaches, aeolian dunes and vermetid-reefs occur only in some sheltered places, mostly on the northeastern coast (Fig. 3).

4.3. Sedimentary deposits

At the IT occur continental and coastal deposits. The continental are constituted by gravel and conglomerates corresponding to talus and alluvial-fans with the morphology entire or partially preserved (Fig. 4). The coastal deposits correspond to beach gravel, sand, conglomerate and sandstone, aeolian sand and vermetid-reefs:

4.3.1. Beach deposits

Present and ancient beach deposits consist of sands, gravels, sandstones and conglomerates. Gravel beaches are found mainly on the western and southern coasts of the island and on the northeastern coast at Valado, Portuguêses and Cabritos beaches (Fig. 3). These beaches are

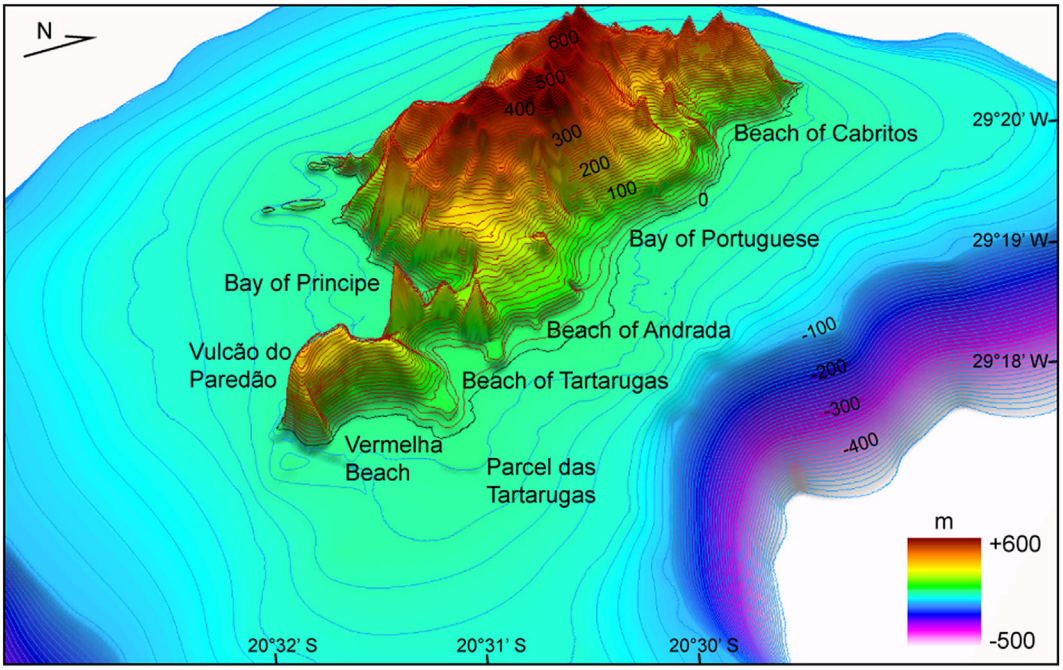

Fig. 8. Topography and bathymetry of IT.

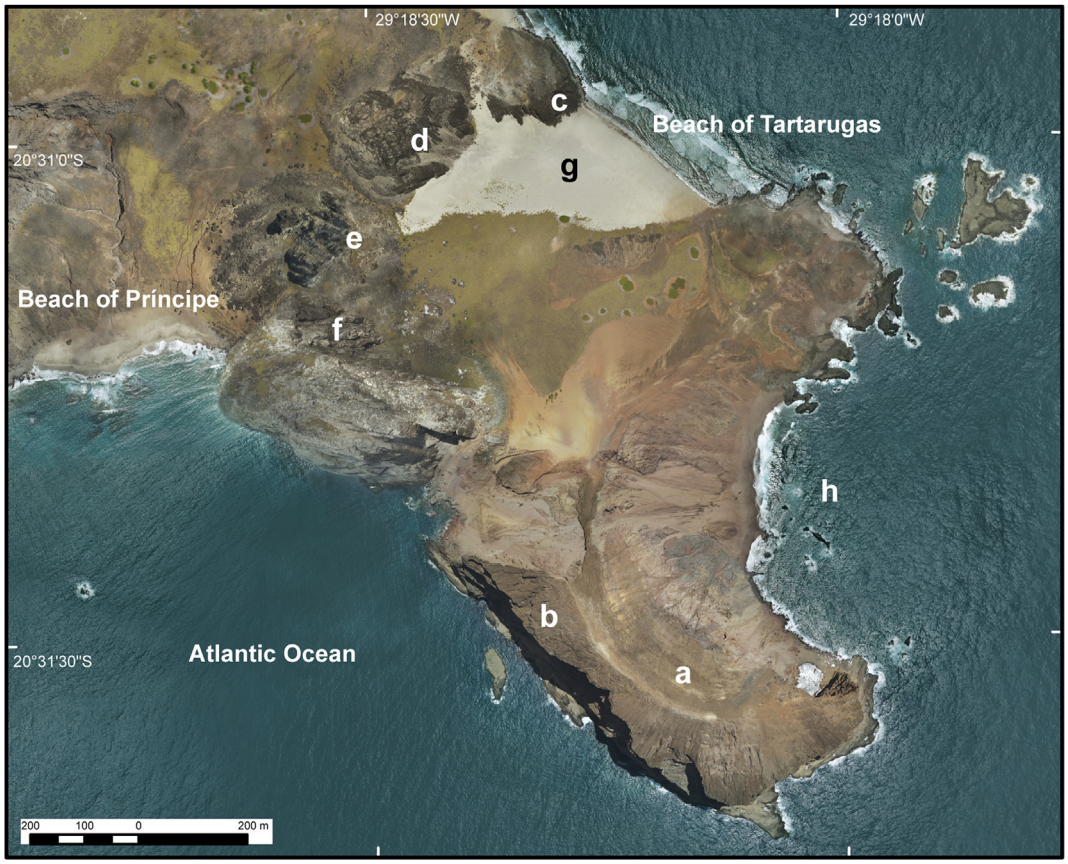

Fig. 9. Vertical aerial view of the eastern end of IT. Note: (a) the crater and (b) the partially preserved depositional slopes of Vulcão do Paredão; and the steep slopes of (c) the southeastern side of Tartarugas, (d) the southern side of Nossa Senhora de Lourdes, (e) the eastern side of Vigia and (f) the northeastern side of the Pão de Açucar hills; (g) the Beach of Tartarugas sedimentary plain and (h) Baixio de Sueste Bay.

characterized by imbricated, rounded, volcanic rock clasts and calcareous bioclasts. A palaeo-gravel beach occurs at Beach of Eme (Almeida, 1961). Holocene conglomerates are present in several places in the intertidal zone along the coast where there is a gravel beach. These conglomerates are clast-supported and contain volcanic rock clasts, calcareous bioclastic and lithoclastic gravel, sand matrix and carbonatic

Fig. 10. Sea cliff and wave-cut terrace (t) at Vulcão do Paredão.

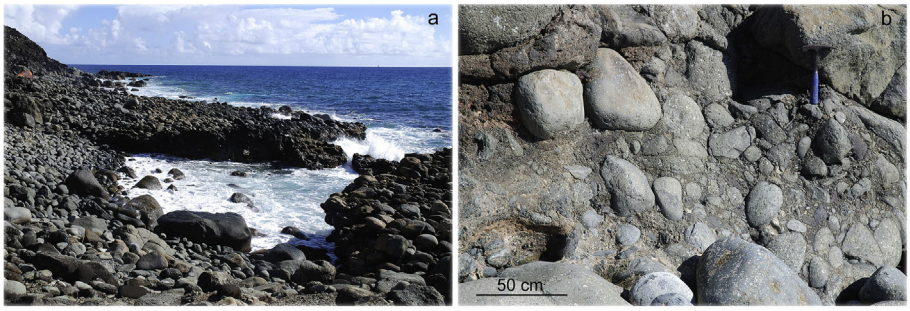

Fig. 11. Gravel beach and palaeo-beach conglomerate at (a) Beach of Portuguêses and (b) on the coast at Valado.

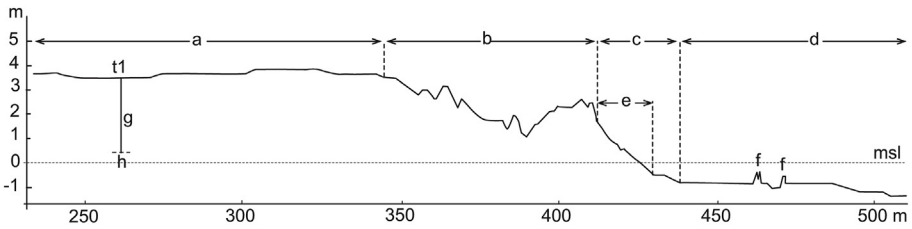

Fig. 12. Topographic profile of at Beach of Tartarugas. (a) Aeolian deflation plain, (b) backshore, (c) beach face, (d) algal reef, (e) beachrock outcrop, (f) palaeo-reef remains, (g) palaeo-beach sand facies, (h) palaeo-algal reef and (t) trench. (msl) Mean sealevel (for location see Fig. 6).

cement (Fig. 11).

Sandy beaches occur mainly along the northeast coast of the island at Cabritos, Andrada, Tartarugas and Vermelha, also named Paredão by Mayer (1957) beaches (Fig. 3); one beach is present on the southwest coast at Príncipe (Fig. 3). The beaches are composed of different proportions of bioclasts and sedimentary and volcanic lithoclasts, and are characterized by a steeply dipping (7°–13°) beach-face and frequently by a berm and a storm-beach at 3.5 m above mean sealevel (Figs. 12 and 13).

Tartarugas ancient beach deposits are 3.2–3.4 m thick and show low-angle cross-stratified with plane-parallel lamination sand facies. These beach deposits overlie an ancient vermetid-reef (Figs. 14 and 15). The sediment consists of lithoclasts and bioclasts, including calcareous red algae, mollusc shells and corals.

Cabritos storm-beach deposits are interfingered with alluvial deposits (Fig. 16). Tartarugas the storm-beach deposits are highly bioturbated by turtle nesting activity and contain calcareous algal and oblate sandstone boulders, transported by high energy waves, measuring a maximum of 3.4 m in the longest axis with a volume of 1 m^3.

In several areas characterized by sandy beaches on the southeastern coast of the island, at Andrada, Vermelha, Parcel das Tartarugas and Tartarugas beaches, outcrops of calcareous sandstone occur (Figs. 3 and 17). The outcrops are concentrated at the southeastern parts of the beaches, suggesting more intense erosion in these sectors. This finding

Fig. 13. Calcareous-algal (c) and sandstone (s) boulders at the storm-beach at Beach of Andrada.

implies a predominant direction of longshore drift from southeast to northwest (Fig. 3).

The sandstones are composed by lithoclast and bioclast gravel and grains and calcareous cement. The gravel bioclasts are mainly calcareous vermetid-reef fragments (Fig. 17). They present conspicuous plane-parallel laminated gravelly sandstone dipping at ~13° eastward (Fig. 17). Therefore, a *sensu stricto* beachrock, because the sub-horizontal plane-parallel laminations correspond to high-regime planar bedforms generated by wave swash and backwash at the beach-face. The sandstones occur at different levels between 0.8 m below and 2.8 m above mean sealevel (Fig. 17).

The beachrocks of Tartarugas are litharenites according to the classification of Folk (1974), and consist of medium to coarse sand grains with carbonatic cement. They are composed of mainly (80%) volcanic rock fragments or monomineralic grains classified as moderately sorted and texturally and mineralogically submature (Fig. 18A and E). Subsidiarily by bioclastic grains, which are predominantly remains of calcareous red algae, echinoderms, gastropods, sponges (Fig. 18B and C), bivalves and foraminifers (e.g. *Homotrema rubrum*). The some grains are coated by acicular aragonitic cement (~20%), and some with fibrous (Fig. 18D and F), bothroidal or equigranular calcite. The secondary porosity generated by dissolution is partially infilled with oxides/hydroxides.

4.3.1.1. Ages of palaeo-beaches. The beach deposits yield Holocene ages younger than 4144 calibrated years before present (cal a BP). Gravel calcareous bioclasts from these deposits yield ages between 4144 and 547 cal a BP and the beachrock composed by calcareous grains and cement was dated to between 2913 and 1990 cal a BP (Table 1).

Fig. 15. Low-angle cross-stratified with plane-parallel lamination sand facies corresponding to palaeo-beach-face deposits at Beach of Tartarugas. (r) Rhizocretion.

4.3.2. Aeolian sands

Aeolian sand deposits occur at beaches exposed to eastern winds. The deposits extend inland for ~0.07 km at Cabritos, 0.2 km at Andrada, limited by the high relief, and ~0.45 km at Tartarugas where a palaeobay is present and the relief is gentler (Figs. 3, 4 and 9). The aeolian deposits were identified as incipient foredunes, climbing dunes

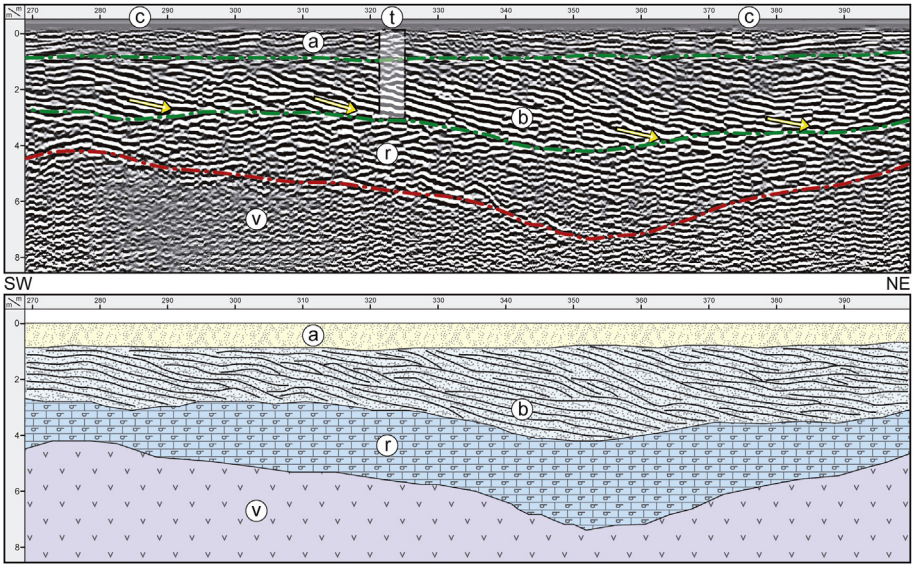

Fig. 14. GPR profile of at Beach of Tartarugas showing interpreted: (a) aeolian and (b) palaeo-beach deposits, which overlie a (r) palaeo-algal-reef. Note the downlap terminations (yellow arrows) indicating beach-face facies progradation over the palaeo-algal-reef surface. (v) Volcanic bedrock, (t) trench and (c) cores (for location see Fig. 6). (For interpretation of the references to colour in this figure legend, the reader is referred to the Web version of this article.)

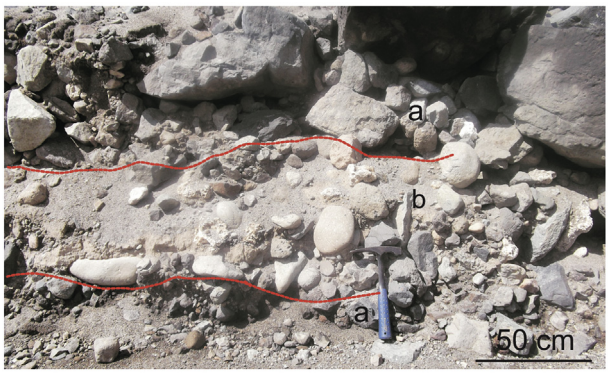

Fig. 16. Interfingered (a) alluvial fan and (b) storm-beach deposits at Beach of Cabritos.

and sand sheets. The aeolian sand consists mainly of calcareous bioclastic grains. At Andrada beach the aeolian deposits occur as thin sand sheets (< 1.5 m) deposited on top of bedrock or alluvial fan deposits (Fig. 19). Toward inland they occur interfingered with alluvial-fan deposits.

Inland Tartarugas beach next to the backshore a sand plain has developed in which sand transport prevails (Fig. 20). At this location aeolian deposits are absent and a gravel lag-deposit containing mostly volcanic clasts, mollusks shells (Table 2), crab remains and rhizocretions occur (Fig. 21). Climbing dunes are present on the steep slopes that surround the Tartarugas coastal plain (Fig. 22).

4.3.3. Vermetid-reefs

Vermetid-reefs occur at Cabritos, Portuguêses, Andrada, Vermelha and Tartarugas beaches (Figs. 3 and 23). These reefs are composed mainly of calcareous vermetid tubes and calcareous algae (Fig. 24). The reefs are found below the spring low-tide level and have surfaces dipping gently (~1°) seaward (Fig. 12).

At Tartarugas and Cabritos beaches, above the presentday surface of the calcareous vermetid-reef pinnacles up to 1.3 m high can be observed (Fig. 23) with a calcareous composition similar to that of the present-day reef and containing conspicuous dissolution surfaces. These pinnacles are interpreted as an ancient vermetid-reef and dated at between 5060 and 3244 cal a BP (Table 1). A palaeo-vermetid-reef was also identified underneath the palaeo-beach deposits at Beach of Tartarugas (Fig. 14): the ages obtained for this reef were 3550–3395 cal a BP (Table 1).

The reef facies mainly consist of calcareous tubes and laminae. The Cabritos ancient reef is composed of approximately 60% bafflestones and framestones of red algae (according to the classification of Embry and Klovan (1971)), with cavities and voids (40%) filled with bioclastic wackestones and packstones (according to the Dunham (1962) classification Fig. 25A) or bladed calcite (Fig. 25E). The micrite matrix of wackestones contains fine-grained sand, and fragments of mainly red coralline algae (Fig. 25D), echinoderms, sponge spicules (Fig. 25F and G), gastropod (Fig. 25B), bryozoans (Fig. 25A), foraminifera (Fig. 25A, C, 25F and 25H) and angular monominerallic terrigenous grains derived from igneous rocks, such as pyroxene, feldspar, and opaque minerals, all in trace amounts.

4.4. Past sealevel changes

Past sealevels were inferred from several indicators: morphological (dead sea cliffs and wave-cut terraces); sedimentary (beach deposits) and biological (sea-urchin hollows and algal-reefs).

Fig. 17. (a) Beach-face sandstone at Beach of Tartarugas with (b) conspicuous plane-parallel laminations and (c) gravel (d) lithoclast and (e) calcareous algal clast that yield ages of 701–547 cal a BP.

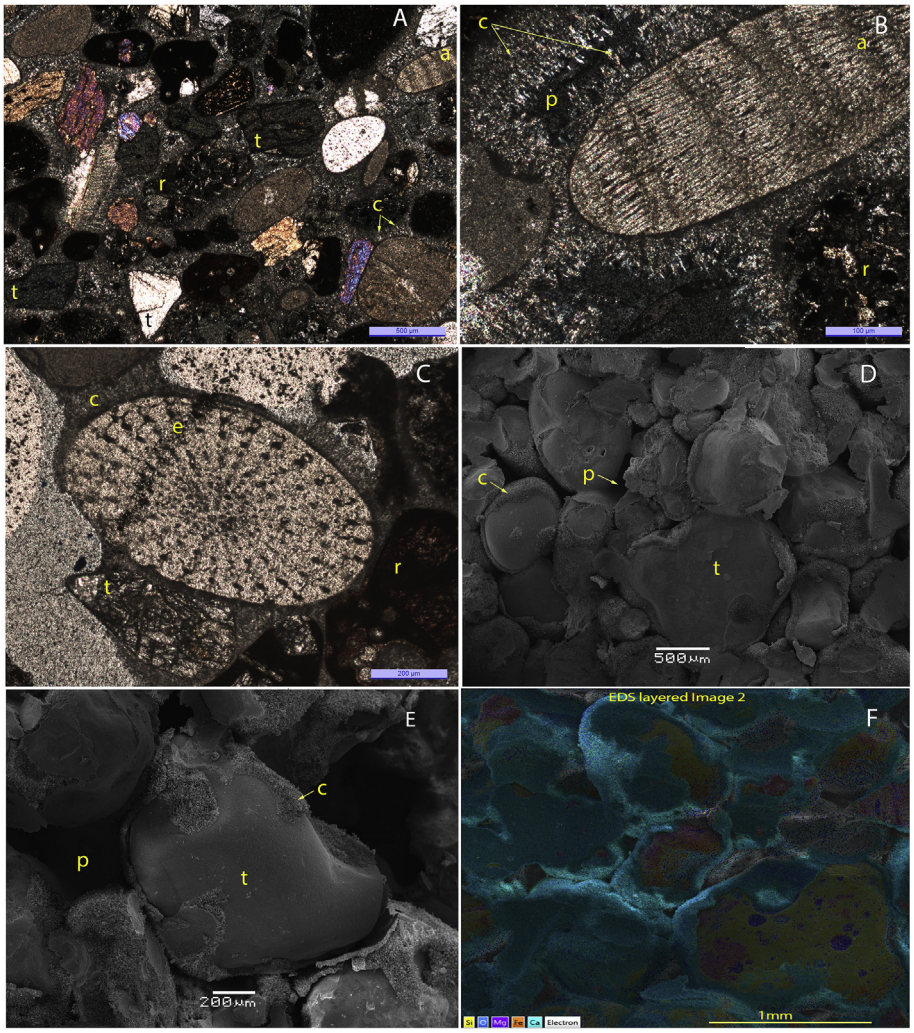

Fig. 18. Beachrock microscopic features: (A) mineralogically submature litharenite, mainly composed of igneous rock fragments (r), terrigenous monominerallic grains (t), and a few bioclasts of (a) red algae, with acicular aragonite (c) early diagenetic pore-lining marine cement (thin section, crossed polarizers); (B) red algae (a) and igneous rock fragment (r), early diagenetic pore-lining marine cement of acicular (radial fibrous) aragonite (c); and low porosity (p) (thin section, crossed polarizers). (C) Echinoid (e), terrigenous (t) and rock-fragment (r) grains, with early diagenetic pore-lining marine cement of acicular (radial fibrous) aragonite (c) (thin section, uncrossed polarizers); (D) and (E) major constituents of beachrock: acicular (isopachous) aragonite cement (c) lining pores (p) between lithoclastic, bioclastic and monominerallic (t) grains, early diagenetic marine phreatic cement (SEM secondary electron image); (F) elemental map sum showing the compositional distinction between terrigenous grains and isopachous aragonite cement of the beach, marine phreatic eodiagenesis. Site: Beach of Tartarugas (for location see Fig. 3). (For interpretation of the references to colour in this figure legend, the reader is referred to the Web version of this article.)

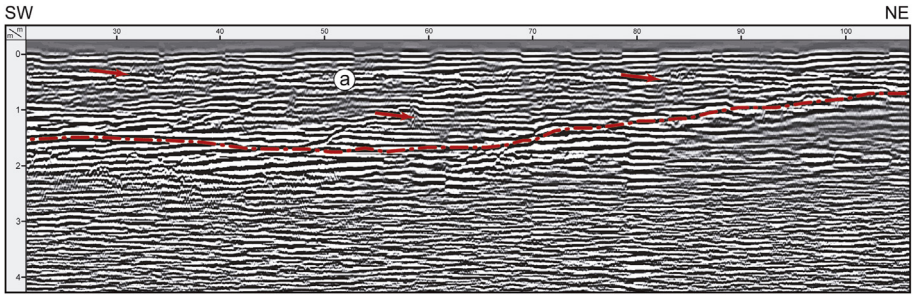

Fig. 19. GPR profile at Beach of Andrada where (a) aeolian sand is deposited over the bedrock. Note the diffraction hyperbolas indicating blocks of the bedrock (red arrows; for location see Fig. 6). (For interpretation of the references to colour in this figure legend, the reader is referred to the Web version of this article.)

4.4.1. Morphological indicators

Dead sea cliffs sculpted into alluvial fan and volcanic deposits (Fig. 4) occur mainly along the northeastern coast of IT. They could have become inactive as a result of coastal progradation generated by a sealevel lowering, as a result of intense sediment supply, or both. The sediment supply is not significant and most of the coast is intensely eroded by waves. Therefore, the presence of dead sea cliffs on the island suggests a sealevel fall (Almeida, 1961).

At several places, e.g., Parcel das Tartarugas, Vulcão do Paredão and the Island of Rachada, wave-cut-terraces occur reaching 200 m wide and 2–4 m above present mean sealevel (Figs. 5 and 10). These terraces are washed by storm waves that remove debris fallen from the cliffs, but most of the time they are not affected by wave action. At Vulcão do Paredão the wave-cut terrace and the sea cliffs are sculpted on stratified tuffs and are not influenced by differential erosion. Therefore, it is probable that these features were formed when the sealevel was higher than at present, as proposed by Almeida (1961).

4.4.2. Sedimentary indicators

The paleosealevels were inferred from the position of ancient beach deposits facies and their contacts, which occur in vertical range from the low-tide level to 3.5 m above the present mean sealevel.

The beach conglomerates were found at several places (Fig. 11) between the low-tide level and the storm wave swash limit, which is the same range of the present gravel beaches. Therefore they may have been deposited when sealevel was similar to or higher than present. The

Fig. 20. Aeolian (s) sand dunes and (d) deflation plain at Beach of Tartarugas.

Table 2
List of mollusk species found at Tartarugas' lag-deposit.

Marine	*Vasula deltoidea* (Lamarck, 1822)
	Gemophos tinctus (Conrad, 1846)
	Monostiolum atlanticum (Coelho, Matthews e Cardoso, 1970)
	Nassarius sp.
	Hipponix antiquatus (Linnaeus, 1767)
	Hipponix grayanus Menke, 1853
	Hipponix aff. *benthophila* (Dal, 1889)
	Hipponix incurvus (Gmelin, 1791)
	Synaptocochlea picta (d'Orbigny, 1847)
	Lottia marcusi (Righi, 1966)
	Diodora arcuata (G. B. Sowerby II, 1862)
	Clathrolucina costata (d'Orbigny, 1846)
	Parvilucina pectinella (C. B. Adams, 1852)
	Mitrella sp.
Terrestrial	*Bulimulus brunoi* (Ihering, 1917)
	Naesiotus arnaldoi (Lanzieri and Rezende, 1971).

age of a bioclast from a conglomerate on the coast at Valado indicates that the maximum age of the deposit is 4144–3889 cal a BP and that sealevel was 0.6 ± 1.4 m above present level after that period (Table 1 and Fig. 26).

The beach-face facies of the beachrock at Beach of Tartarugas occur in vertical range since the beach-step, in contact with the present algal-reef at the base to the present beach berm top. This range is coincident with the present homologous beach-face facies range, which occur at 0.8 m below present mean sealevel until the beach-berm top at 2.5 m above present mean sealevel. Assuming that no changes on oceanographic conditions the beachrock facies indicate a paleosealevel of 0.0 ± 0.2 m (Fig. 17c). The age of a bioclast from this facies that indicates the maximum depositional age of the facies is 701–547 cal a BP (Table 1).

Beach-face facies at Parcel das Tartarugas occur at 2.8–2.2 m above mean sealevel and at Beach of Andrada at 1.3–0.7 m above mean sealevel. The homologous present beach-face facies occur from the beach-step, in contact with the algal-reef, at 0.8 m below mean sealevel, to the present beach-berm top at 2.5 m above mean sealevel. Therefore the beach-face facies indicates paleosealevels of 1.4 ± 1.7 m at Parcel das Tartarugas and 0.2 ± 1.4 m at Beach of Andrada. These beachrock yield ages between 2490 and 1990 cal a BP (Table 1), but they are only approximated depositional age because the dated sample is composed by bioclasts older than the deposit and cement younger than the depositional age (Angulo et al., 2013).

Fig. 21. Rhizocretions fragments from the Tartarugas gravel lag-deposit. Note the ramification and the smooth surface at the inner part of the tube.

A more precise level estimate can be obtained by considering the basal contact of the sand beach-face facies with the palaeo-algal-reef surface at beach of Tartarugas (Figs. 12 and 14). This contact is 1.1–1.5 m above the present homologous contact (Fig. 12), suggesting that the sealevel was 1.3 ± 0.2 m higher than the present one.

Fig. 22. Climbing dunes (c) at Beach of Tartarugas.

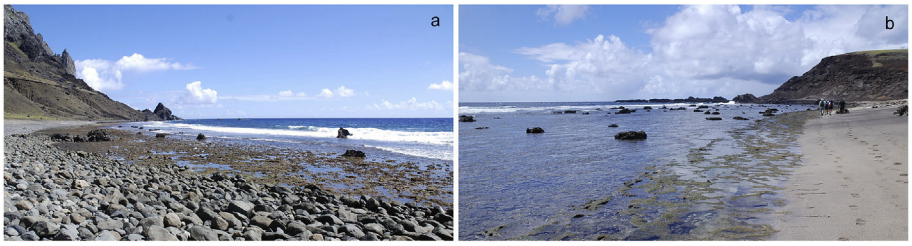

Fig. 23. (a) Cabritos and (b) Tartarugas vermetid-reefs, at low-tide. The present reef surface is at the low-tide level and the ancient reef remains are emerged during low-tide.

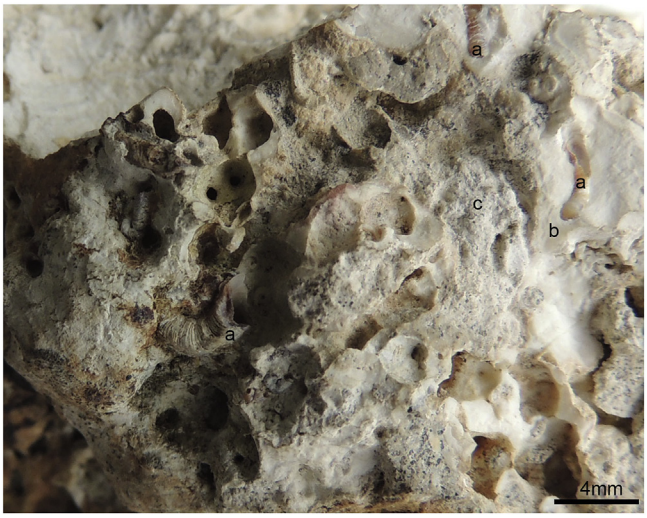

Fig. 24. Cabritos ancient vermetid-reef (Sample C1, Table 1). (a) Vermetid tube, (b) calcareous overgrowth and (c) cemented grains.

The ± 0.2 m precision to estimate palaeosealevel was possible because present basal contact of the sand beach-face with the algal-reef surface correspond to a horizontal line along the beach-arc levelled at the upper-limit of grows of the algal-reef species (Fig. 23).

The age of a bioclast from the bottom of this facies indicates that the maximum depositional age of the unit is 3620–3605 cal a BP (Table 1).

4.4.3. Biological indicators

At several places dense groups of well-preserved sea-urchin hollows were observed up to 1.3 m above their homologous present living position (Fig. 27). The low level of abrasion suggests that the holes were formed during the Holocene when the sealevel was at least 1.3 m above present one.

The best indicators occurring are the palaeo-algal-reefs. As described, two different occurrences have been found: (a) reef remains that have experienced intense dissolution and erosion that are elevated above the present living algal-reef (Fig. 23) and (b) reef remains that occur under palaeo-beach deposits (Fig. 14).

The algal-reef remains at Cabritos and Tartarugas beaches (Fig. 23) are as much as 1.3 m above the present algal-reef surface. The ages of these structures are between 5060 and 3244 cal a BP (Table 1), indicating that at that time the sealevel was at least 1.3 m above its present level (Fig. 26).

The surface of the palaeo-algal-reef identified under the palaeo-beach deposits at Beach of Tartarugas (Fig. 14) is at 1.1–1.5 m above the present living algal-reef and has an age of 3550–3395 cal a BP (Fig. 23b and Table 1), indicating that the time the reef was formed, the sealevel was 1.3 ± 0.2 m higher than at present (Fig. 26).

5. Discussion and conclusions

All evidence for Holocene sealevels are higher than the present and the ages range between 5.06 and 0.55 ka (Fig. 26). The altitude and ages of the reconstructions are in good agreement with hindcast model curves (Milne et al., 2005) and the empirical sealevel envelope for the mainland eastern and northeastern Brazilian coast presented by Angulo et al. (2006). (For a discussion about different proposed empiric relative sealevel curves, see Angulo et al., 2006). This agreement shows that no significant vertical movement has taken place during the last 5.1 ka and that a higher sealevel corresponds to a eustatic sealevel change. However, the ancient algal-reef at Beach of Tartarugas, which is the most precise indicator, that sealevel was 0.5–0.9 m lower than eustatic elevation at that time (3550–3395 cal a BP, Fig. 26) suggesting the Island subsidence reported at Fernando de Noronha archipelago (Angulo et al., 2013).

No evidence of Pleistocene sealevels higher than present was detected at the Island. This result is quite different from the mainland Brazilian coastal zone, where conspicuous evidence of Pleistocene sea levels higher than present can be found (e.g. Isla and Angulo, 2015). The absence of evidence can be attributed to intense coastal erosion and island subsidence. Considering that the Sangamonian highstand is not present, and the mid-Holocene highstand is lower than at the continent, it is possible to assume that the volcanic edifice is under a long-term subsidence.

The geomorphological evolution of the IT can be summarized as follows. A volcanic edifice more than 5500 m high was built during the

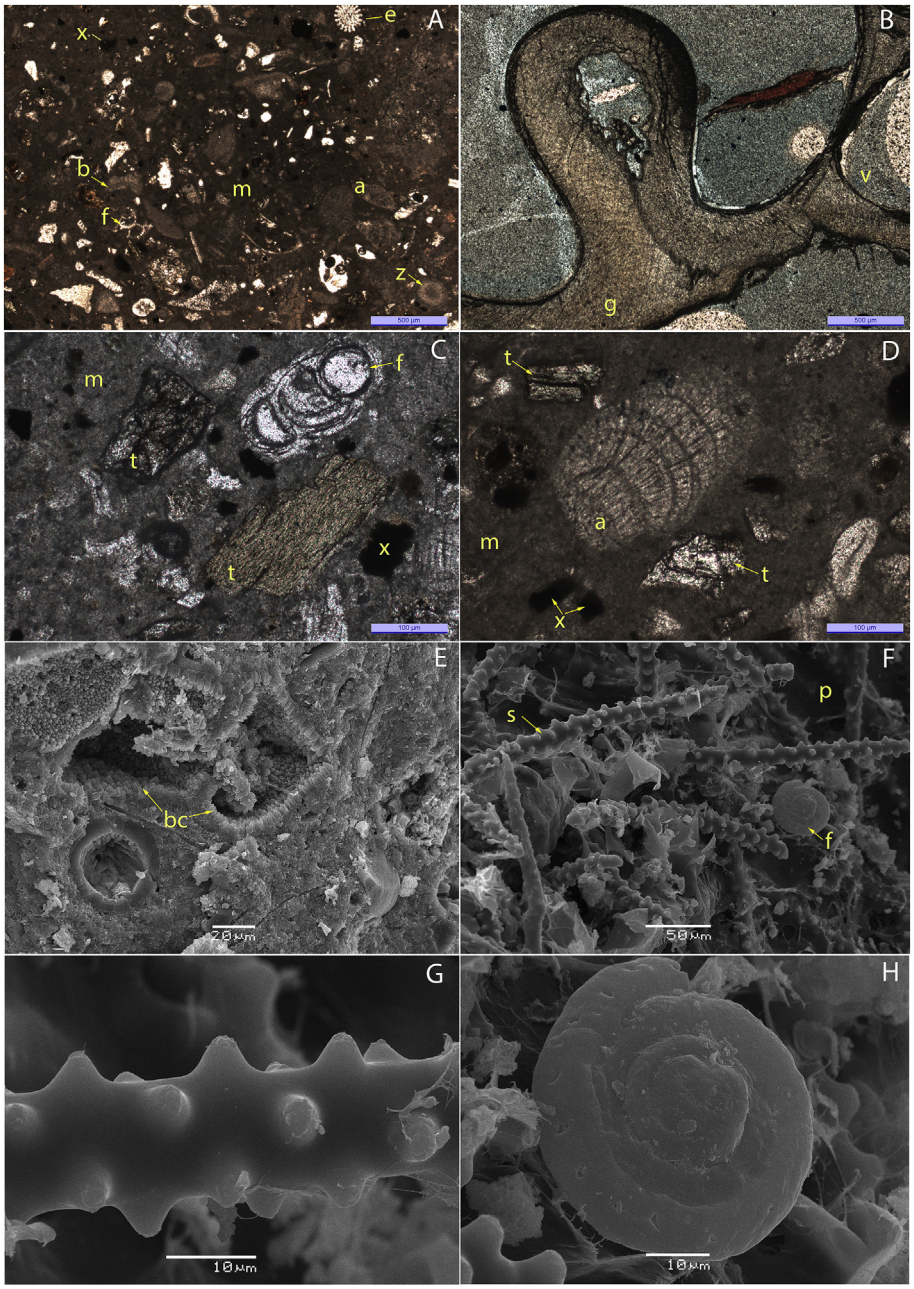

Fig. 25. Vermetid-reef micro features: A) bioclastic wakestone that infill reef cavities and vugs (thin section, crossed polarizers); B) unidentified gastropod (left) and vermetid (right) in contact (thin section, uncrossed polarizers); C) foraminifer and terrigenous grain in micrite matrix of wakestone that infill the reef cavities and vugs. Note ferruginous oxides/hydroxides telodiagenetic cement infilling secondary porosity (thin section, uncrossed polarizers); D) red algae and terrigenous grains on micrite matrix of infilling reef cavities and vugs (thin section, uncrossed polarizers); E) reef vugs lining by bladed calcite (SEM secondary electrons image); F) monoaxonid spicules of sponges and foraminifer; packstone with micrite matrix (SEM secondary electron image); G) detail of a monoaxonid spicule of sponge (SEM secondary electron image); H) Spirillinidae foraminifer (SEM secondary electrons image). Key: (a) red algae, (b) indeterminate bioclasts, (bc) bladed calcite, (e) echinoid, (f) foraminifer, (g) gastropod, (m) micrite matrix, (p) secondary porosity, (s) spicules of sponge, (t) terrigenous grain, (v) vermetid, (**z**) bryozoan. Secondary porosity filled by iron oxides/hydroxides (**x**), of wakestone that infill the reef cavities and vugs. Site: Bach of Cabritos (for location see Fig. 3). (For interpretation of the references to colour in this figure legend, the reader is referred to the Web version of this article.)

late Pliocene to early Pleistocene (2.9–2.3 Ma) by several eruptions, and forming the Trindade Complex and Desejado sequence. After this time intense sub-aerial and coastal erosion reduced most of the upper part of the volcanic edifice. During Pleistocene lowstands coastal erosion removed the volcanic edifice to 100 m below present sealevel, as indicated by the 50 km^2 island shelf (Fig. 8). The IT represents the remaining 17% of the emergent volcano area. During Pleistocene sealevel lowstands alluvial fans were formed and this morphology preserved by lava flows and pyroclastic deposits of Middle to Late Pleistocene age (170 ka). During the last Interglacial highstand (c.a. 120 ka, MIS Ve) intense coastal erosion removed the distal parts of the alluvial fans (Fig. 4). At that time the entire coast must underwent intense erosion and probably subsidence, as suggested by the absence of Pleistocene coastal deposits, common on the continental Brazilian coast. The eastern coast of the IT was defined by high sea cliffs sculpted into the Desejado volcanic rock hills (Fig. 9). Subsequently, the Vulcão do Paredão volcanic cone was formed, when sealevel was lower than at present during the Late Pleistocene to early Holocene. During the Holocene sealevel highstand, since7 ka to present (Fig. 26), the volcanic cone was partially eroded and a bay formed at Beach of Tartarugas coast (Fig. 9). At the beginning of this highstand (7–5 ka), an algal-reef grew at the ancient Tartarugas Bay and the beach-sand deposits prograded until the bay was filled in (Fig. 14). The ages of the ancient algal-reef and the beach-sand deposits indicate prograding rates of 0.41–0.46 m per year during the last 3.6–3.4 kyr. During the sealevel maximum sea cliffs were active and wave-cut terraces, included Vulcão do Paredão one, were sculpted. In the mid–late Holocene, talus and alluvial fan deposits were interfingered with beach and aeolian deposits, e.g., at Cabritos and Tartarugas (Fig. 16). During the sealevel lowering the sea cliffs became inactive, such as on the coast at Valado and Cabritos (Fig. 4) and the ancient algal-reefs were eroded (Fig. 23). Currently, beach erosion and aeolian deflation prevail, indicating a low sediment supply.

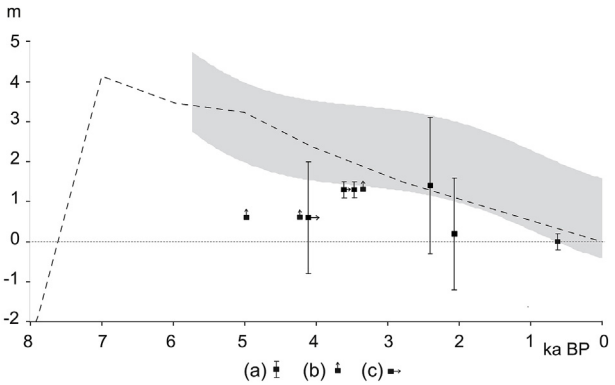

Fig. 26. Holocene sealevel reconstructions for the IT and sealevel envelope (grey area) for the eastern Brazilian coast between 07°S and 26°S (after Angulo et al., 2006), and sealevel behaviour predicted for the latitude of Rio de Janeiro by geophysical simulations (dashed line, after Milne et al., 2005). (a) Maximum and minimum heights, (b) minimum height and (c) maximum age.

Fig. 27. Sea-urchin hollows 1.3 m above their homologous present living position at Parcel das Tartarugas.

Acknowledgements

We are grateful to Marinha do Brasil (Brazilian Navy) for making this research possible and to Conselho Nacional de Pesquisa– CNPq (Brazilian Research Council) and Comissão Interministerial para os Recursos do Mar– CIRM (Inter-Ministry Commission for Ocean Resources) for their financial support though projects numbers 557141/2009-5, 457714/2013-1 and 442865/2015-5. We extend special thanks to Capitão-de-Fragata Rodrigo Otoch Chaves in charge of the Trindade Island Scientific Research Program - Protrindade, to the NDCC Almirante Saboia ship commandant Contra-Almirante Valter Citavicius Filho, immediate Capitão-de-Fragata César Vidal, doctor Capitão-de-Corveta Felipe Castro and all the Hipo crew; and all the Helicopter Esquadrão HU-2 pilots, particularly Cap-de-Fragata Silvio Fernando Ferreira and Cap-de-Corveta Anderson Veras Marques, for support, care and friendship. We wish to thank all our scientific colleagues who participated in the XV-Protrindade expedition, and the island base commandant and the crew, with special mention to our field trip guides. We are also grateful to the Center of Electronic Microscopy of UFPR for providing facilities, to MSC. Augusto Luiz Ferreira Junior for his help with mollusks taxonomy and to Dr. Lauro J. Calliari of FURG for provides a Total Station. We are grateful to the anonymous reviewers for the contribution to improve de manuscript. RJA, MCS, EGB, LAF and LHSO are sponsored by CNPq fellowships (303940/2014-0, 305691/2014-7, 303433/2017-5, 383136/2015-6). RJA is also sponsored by Fundação Araucária senior fellowship (45725).

References

Abreu, V.S., Neal, J., Vail, P.R., 2010. Integration of sequence stratigraphy concepts. In: Abreu, V.S., Neal, J., Bohacs, K.M., Kalbas, J.L. (Eds.), Sequence Stratigraphy of Siliciclastic Systems – the ExxonMobil Methodology: Atlas of Exercises, pp. 209–224.
Almeida, F.F.M., 1955. Geologia e petrologia do arquipélago de Fernando de Noronha. Monografia, 13. Departamento Nacional da Produção Mineral, Rio de Janeiro, pp. 181.
Almeida, F.F.M., 1961. Geologia e petrologia da ilha de Trindade. Monografia, 18. Departamento Nacional de Produção Mineral, Rio de Janeiro, pp. 197 1map.
Alves, R.J.V., 1998. Ilha da Trindade & Arquipélago Martin Vaz: um ensaio geobotânico. Serviço de Documentação da Marinha, Rio de janeiro, pp. 144.
Angulo, R.J., Lessa, G.C., Souza, M.C., 2006. A critical review of mid- to late-Holocene sealevel fluctuations on the eastern Brazilian coastline. Quat. Sci. Rev. 25, 486–506.
Angulo, R.J., Souza, M.C., 2014. Conceptual review of Quaternary coastal paleo-sea level indicators from Brazilian coast. Quat. Environ. Geosci. 05 (2), 1–32 (in Portuguese).
Angulo, R.J., Souza, M.C., Fernandes, L.A., Disaró, S.T., 2013. Quaternary sea-level changes and aeolianites in the Fernando de Noronha archipelago, northeastern Brazil. Quat. Int. 305, 15–30.
Barboza, E.G., Rosa, L.C.C., Caron, F., 2014. Metodologia de Aquisição e Processamento em Dados de Georradar (GPR) nos Depósitos Quaternários da Porção Emersa da Bacia de Pelotas. In: VI Simpósio Brasileiro de Geofísica, 2014, Porto Alegre-RS. Resumos Expandidos, vol 1. pp. 1–6.
Barboza, E.G., Rosa, M.L.C.C., Hesp, P.A., Dillenburg, S.R., Tomazelli, L.J., Ayup-Zouain, R.N., 2011. Evolution of the Holocene coastal barrier of pelotas basin (southern Brazil) - a new approach with GPR data. J. Coast Res. 64, 646–650 SI.
Catuneanu, O., Abreu, V.S., Bhattacharya, J.P., Blum, M.D., Dalrymple, R.W., Eriksson, P.G., Fielding, C.R., Fisher, W.L., Galloway, W.E., Gibling, M.R., Giles, K.A., Holbrook, J.M., Jordan, R., Kendall, C.G.S.T.C., Macurda, B., Martinsen, O.J., Miall, A.D., Neal, J.E., Nummedal, D., Pomar, L., Posamentier, H.W., Pratt, B.R., Sarg, J.F., Shanley, K.W., Steel, R.J., Strasser, A., Tucker, M.E., Winker, C., 2009. Towards the standardization of sequence stratigraphy. Earth Sci. Rev. 92, 1–33.
Cordani, U.G., 1970. Idade do vulcanismo no oceano Atlântico Sul. Boletim do Instituto de Geociências e Astronomia da Universidade de São Paulo 1, 9–75.
Daniels, J., Roberts, R., Vendl, M., 1995. Ground penetrating radar for the detection of liquid contaminants. J. Appl. Geophys. 33, 195–207.
Darwin, C., 1839. Journal of Researches into the Geology and Natural History on the Various Countries Visited by H.M.S. Beagle. Henry Colburn, London, pp. 615 Under the Command of Captain Fitzroy, R.N. from 1832 to 1836.
DHN - Diretoria de Hidrografia e Navegação, 1971. Carta náutica Ilha da Trindade n. 21, scale 1:15,000.
Dunham, R.J., 1962. Classification of carbonate rocks according to their depositional texture. In: In: Ham, W.E. (Ed.), Classification of Carbonate Rocksea Symposium, vol 1. American Association of Petroleum Geologists Memoir, Tulsa, OK, pp. 108–121.
Embry, A.F., Klovan, J.E., 1971. A late Devonian reef tract on northeastern Banks island, N.W.T. Bull. Can. Petrol. Geol. 19, 730–781.
Folk, R.L., 1974. Petrology of Sedimentary Rocks. Hemphills, Austin, Texas, pp. 104.
Gass, I.G., 1967. Geochronology of the Tristan da Cunha group of islands. Geol. Mag. 104 (2), 160–170.
Hekinian, R., Juteau, T., Gràcia, E., Sichler, B., Sichel, S., Udintsev, G., Appriou, al, R., Ligi, M., 2000. Submersible observations of equatorial Atlantic mantle: the St. Paul Fracture zone region. Mar. Geophys. Res. 21, 529–556.
Isla, F.I., Angulo, R.J., 2015. Tectonic processes along the South America coastline derived from Quaternary marine terraces. J. Coastal Res. 32 (4), 840–852.
Lobo, B., 1919. Conferencia sobre a Ilha da Trindade. Arq. Mus. Nac. 22, 105–169.
Marinha do Brasil, 2011. Boletim Climatológico Nº 14. Centro de Hidrografia da Marinha, relatório interno. pp. 15.
Mayer, E.M., 1957. Trindade, Ilha Misteriosa Dos Trópicos. Livraria Tupã Editora, Rio de Janeiro, pp. 159.
Milne, G.A., Long, A.J., Bassett, E., 2005. Modeling Holocene relative sea-level observations from the Caribbean and south America. Quat. Sci. Rev. 24 (10–11), 1183–1202.
Mitchum Jr., R.M., Vail, P.R., Sangree, J.B., 1977. Seismic stratigraphy and global changes of sea level, Part 6: stratigraphy interpretation of seismic reflection patterns in depositional sequences. In: In: Payton, C.E. (Ed.), Seismic Stratigraphy — Applications to Hydrocarbon Exploration, vol 26. AAPG, Tulsa, pp. 117–133.
Neal, A., 2004. Ground-penetrating radar and its use in sedimentology: principles, problems and progress. Earth Sci. Rev. 66, 261–330.
Nunn, P.D., 1984. Occurrence and ages of low-level platforms and associated deposits on South Atlantic coasts: appraisal of evidence for regional Holocene high sea-level. Prog. Phys. Geogr. 8, 32–58.
Payton, C.E., 1977. Seismic Stratigraphy — Applications to Hydrocarbon Exploration. AAPG, Tulsa, pp. 516 (Memoir # 26).
Stuiver, M., Reimer, P.J., 1986. A computer program for radiocarbon age calibration. Radiocarbon 28, 1022–1030.
Vail, P.R., 1977. Seismic stratigraphy and global changes of sea level. In: AAPG seismic stratigraphy Applications to hydrocarbon exploration. AAPG Memoir 26, 83–98.